PERGAMON

International Journal of Heat and Mass Transfer 45 (2002) 3181–3188

International Journal of HEAT and MASS TRANSFER

www.elsevier.com/locate/ijhmt

Forced convection in horizontal porous channels with hydrodynamic anisotropy

G. Degan [a,*], S. Zohoun [a], P. Vasseur [b]

[a] *LERTI-CPU, Université Nationale du Bénin, Boite Postale 2009, Cotonou, Benin*

[b] *Ecole Polytechnique, University of Montreal, 6079 ''Centre-Ville'', Montreal, Canada H3C 3A7*

Received 24 August 2001; received in revised form 24 October 2001

Abstract

This paper presents an exact solution for fully developing forced convective flow in parallel-plate horizontal porous channels with an anisotropic permeability whose principal axes are oriented in a direction that is oblique to the gravity vector. A constant heat flux is applied on the channel side walls. Basing this analysis on the generalized Brinkman-extended Darcy model which allows the satisfaction of the no-slip boundary condition on solid wall, it is found that anisotropic parameters K^* and φ have a strong influence on the flow fields and heat transfer rate, in the limiting case of low porosity media ($Da \to 0$). The results indicate that a maximum (minimum) heat transfer rate is reached when the orientation of the principal axis with higher permeability of the anisotropic porous matrix is parallel (perpendicular) to the vertical direction.

1. Introduction

Convective heat transfer in porous media has received increasing interest over the last 20 years, due its numerous applications in geophysics and energy-related systems. Convection in ducted flow may occur in many applications, such as heat exchangers, chemical processing equipment, transport of heated or cooled fluids, solar collectors and micro-electronic cooling. Buoyancy effects distort the velocity and temperature profiles relative to the forced convection case. This phenomenon is of substantial significance because it may strongly affect wall friction, pressure drop, heat transfer, occurrence of extreme temperatures and stability of the flow.

In channel flow, enhancement of heat transfer by insertion of solid matrices has been analyzed [1,2] and studied experimentally [3] for relatively low permeabilities. In treating these flows, uniform velocity is generally assumed across the channel. However, for relatively high porosities and permeabilities (which are desirable for pressure drop consideration), a non-uniform velocity distribution is expected near the wall. This affects the heat transfer rate from or to the walls. Kaviany [4] tudied laminar convective flow through a porous channel bounded by two parallel plates maintained at a constant and equal temperature. On the basis of the modified Darcy model for transport of momentum, this author has demonstrated that the Nusselt number for fully developed fields increases with an increase of the porous media shape parameter. Nakayama et al. [5] extended Kaviany's analysis to the case of constant heat flux specified to the walls, employing the Brinkman-extended Darcy model, to study the effect of the boundary viscous frictional drag on hydrodynamic and heat transfer characteristics. Recently, Haajizadeh and Tien [6] have investigated combined natural and forced convective flows through a horizontal porous channel connecting two reservoirs and found that a small rate of throughflow has a significant effect on the temperature distribution and the heat transfer across the channel.

So far, theoretical and experimental investigations on the topic have usually been concerned with isotropic porous media. However, in several applications the porous materials are anisotropic. The inclusion of more physical realism in the matrix properties of the medium

* Corresponding author. Tel.: +229-955-251; fax: +229-360-199.

E-mail address: gdegan@syfed.bj.refer.org (G. Degan).

0017-9310/02/$ - see front matter
PII: S0017-9310(02)00032-7

Nomenclature

a, c	constants, Eq. (9)
Da	Darcy number, K_1/h^2
f	wall friction factor, $\tau_w/(1/2\varrho\overline{u}^2)$
h	half channel height
$\underline{k}$	thermal conductivity
$\overline{\overline{K}}$	flow permeability tensor, Eq. (4)
K_1, K_2	flow permeability along the principal axes
K^*	anisotropic permeability ratio, K_1/K_2
p'	fluid thermodynamic pressure
q_w	wall uniform heat flux
Nu	Nusselt number, Eq. (32)
Re	Reynolds number, $\overline{u}h/\nu$
T'	fluid temperature
ΔT	temperature scale, $q_w h/k$
$\vec{V}$	seepage velocity
u, v	dimensionless velocity components in x, y directions
$\overline{u}$	average velocity
x	dimensionless horizontal coordinate
y	dimensionless vertical coordinate

Greek symbols

α	constant, Eq. (18)
β	thermal expansion coefficient of the fluid
θ	dimensionless temperature profile
φ	inclination of the principal axis
μ	dynamic viscosity of the fluid
ν	kinematic viscosity of the fluid
λ	relative viscosity, μ_{eff}/μ
ϱ	density of the fluid
$(\varrho c)_f$	heat capacity of the fluid
τ_w	wall shear stress

Superscript

$'$	dimensional quantities

Subscripts

m	refers to bulk mean
w	refers to wall

is important for the accurate modeling of the anisotropic media. Anisotropy, which is generally a consequence of a preferential orientation or asymmetric geometry of the grain or fibers, is in fact encountered in numerous systems in industry and nature. Example include fibrous materials, geological formations, oil extraction, some biological materials, and dendritic regions formed during solidification of binary alloys. Despite its broad range of applications, convection in such anisotropic porous media has received relatively little attention. The first study of natural convection in anisotropic porous channels with principal axes of permeability coincident with the gravity vector seems to be that by Nilsen and Storesletten [7]. Assuming that the horizontal channel walls are impermeable and non-uniformly heated to establish a linear temperature distribution, critical Rayleigh numbers were derived for the onset of convection and the influence of anisotropic permeability are seen significant. Recently, Degan and Vasseur [8] conducted an analytical study on the aiding convection in parallel vertical porous channels with an anisotropic permeability whose principal axes are oriented in a direction which is oblique to the gravity vector. Using the generalized Brinkman-extended Darcy model which allows the no-slip boundary condition on solid wall, to be satisfied, both flow reversal and limiting cases of low and high porosity media for natural and forced convection are considered to demonstrate the influence of the anisotropy on the flow and heat transfer characteristics.

The aim of the present analysis is to study forced convective flows in parallel-plate horizontal porous channels with an anisotropic permeability whose principal axes are arbitrary oriented, as it is seen in nature and for many realistic applications. The convective flow is induced by two horizontal bounding walls heated by a constant heat flux. On the basis of the generalized Brinkman-extended Darcy model, the effects of anisotropic parameters of the porous matrix on velocity and temperature fields and heat transfer rate are investigated in detail.

2. Mathematical formulation and resolution

The physical model illustrating the problem considered here in Fig. 1 consists of a two-dimensional horizontal parallel-plate porous channel of height $2h$, whose the upper and lower plates are impermeable and heated by a constant heat flux $q_w = k\partial T'/\partial y'$. The axial and

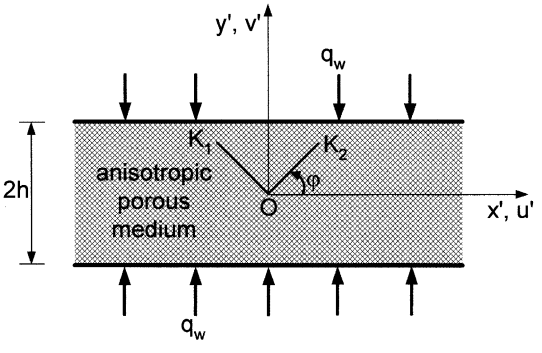

Fig. 1. Physical situation and coordinate system.

transverse coordinates are respectively x' and y', the latter being measured vertically upwards from the channel centerline. The porous medium is anisotropic in flow permeability, the permeabilities along the two principal axes of the porous matrix are denoted by K_1 and K_2. The anisotropy of the porous medium is characterized by the permeability ratio $K^* = K_1/K_2$ and the orientation angle φ, defined as the angle between the horizontal direction and the principal axis with the permeability K_2. The porous medium is saturated with an incompressible viscous fluid that is in local thermodynamic equilibrium with the solid matrix.

Under the above approximations, the equations governing the conservation of mass, momentum and energy (for steady forced convective flow) in an anisotropic porous medium can be written as follows [9,10]:

$$\nabla \cdot \vec{V}' = 0, \tag{1}$$

$$\vec{V}' = \frac{\overline{\overline{K}}}{\mu}\left(- \nabla p' + \mu_{\text{eff}} \nabla^2 \vec{V}' \right), \tag{2}$$

$$(\varrho c)_{\text{f}} \nabla \cdot (\vec{V}' T') = k \nabla^2 T', \tag{3}$$

where $\vec{V}'$ is the superficial flow velocity, T' the temperature, $(\varrho c)_{\text{f}}$ the heat capacity of the fluid, μ the dynamic viscosity, p' the pressure, μ_{eff} apparent dynamic viscosity for Brinkman's model, k the thermal conductivity, ϱ the density. The symmetrical second-order permeability tensor $\overline{\overline{K}}$ is defined as

$$\overline{\overline{K}} = \begin{bmatrix} K_1 \sin^2 \varphi + K_2 \cos^2 \varphi & (K_2 - K_1) \sin \varphi \cos \varphi \\ (K_2 - K_1) \sin \varphi \cos \varphi & K_2 \sin^2 \varphi + K_1 \cos^2 \varphi \end{bmatrix}. \tag{4}$$

Assuming that when the flow is fully developed in the channel, the axial (x'-direction) velocity depends on the transverse coordinate y' (i.e., $u' = u'(y')$) and then from the continuity equation, the transverse velocity component must be zero ($v' = 0$). The temperature is assumed to be a function of x' plus a function of y'. No assumptions are made with regard to the pressure variation (which, in fact, is not found to be a linear function of x' as it is often assumed). So, governing equations (1)–(3) may be reduced as

$$\frac{\mathrm{d}u'}{\mathrm{d}x'} = 0, \tag{5}$$

$$0 = -\frac{\partial p'}{\partial x'} + \mu_{\text{eff}} \frac{\mathrm{d}^2 u'}{\mathrm{d}y'^2} - \frac{\mu}{K_1} a u', \tag{6}$$

$$0 = -\frac{\partial p'}{\partial y'} + \frac{\mu}{K_1} c u', \tag{7}$$

$$u' \frac{\partial T'}{\partial y'} = \frac{k}{(\varrho c_{\text{p}})_{\text{f}}} \frac{\partial^2 T'}{\partial y'^2}, \tag{8}$$

where

$$a = \sin^2 \varphi + K^* \cos^2 \varphi, \quad c = \frac{1}{2}(1 - K^*) \sin 2\varphi. \tag{9}$$

Since the velocity and temperature fields are symmetric about the channel centerline, only the upper half of the duct will be taken in consideration. The appropriate boundary conditions prevailing for previous governing equations (5)–(8) are

$$y' = 0: \quad \frac{\mathrm{d}u'}{\mathrm{d}y'} = 0, \quad \frac{\partial T'}{\partial y'} = 0, \tag{10}$$

$$y' = h: \quad u' = 0, \quad \frac{\partial T'}{\partial y'} = \frac{q_{\text{w}}}{k}. \tag{11}$$

Upon integrating the energy equation (8) once over the range $0 \leqslant y' \leqslant h$, one can have

$$u'_{\text{m}} \frac{\mathrm{d}T'_{\text{m}}}{\mathrm{d}x'} = \frac{1}{(\varrho c_{\text{p}})_{\text{f}}} \frac{q_{\text{w}}}{h}, \tag{12}$$

where u'_{m} and T'_{m} are the fluid bulk mean velocity and the fluid mean temperature, respectively. The foregoing equation may be used to eliminate $\partial T'/\partial x' = (\mathrm{d}T'_{\text{m}}/\mathrm{d}x')$ from Eq. (8) to give

$$\frac{u'}{u'_{\text{m}}} = \frac{kh}{q_{\text{w}}} \frac{\partial^2 T'}{\partial y'^2}. \tag{13}$$

Taking hRe (and h), $\overline{u}$, $(\varrho \overline{u}^2)$ and $\Delta T = q_{\text{w}} h/k$ as respective dimensional scales for length x' (and y'), velocities, pressure and temperature, the governing equations (5)–(8) may be written in non-dimensional form as

$$\frac{\mathrm{d}u}{\mathrm{d}x} = 0, \tag{14}$$

$$\frac{\mathrm{d}^2 u}{\mathrm{d}y^2} - \frac{\alpha^2}{\lambda} u = \frac{1}{\lambda} \frac{\partial p}{\partial x}, \tag{15}$$

$$\frac{\partial p}{\partial y} = \frac{c}{Da\,Re} u, \tag{16}$$

$$\frac{u}{u_{\text{m}}} = \frac{\partial^2 \theta}{\partial y^2}, \tag{17}$$

where

$$\alpha^2 = \frac{a}{Da} \tag{18}$$

and the dimensionless temperature is such that $\theta = (T' - T'_{\text{w}})/\Delta T$ (T'_{w} being the local wall temperature).

In the above equations, $Da = K_1/h^2$ is the Darcy number, $Re = \overline{u}h/\nu$ the Reynolds number and $\lambda = \mu_{\text{eff}}/\mu$ the relative viscosity for which the value in the present study is taken, as a first approximation, equal to unity (i.e., $\mu_{\text{eff}} \approx \mu$).

Eliminating the pressure from Eqs. (15) and (16) in the usual way and making use of Eq. (14), one may have

$$\frac{\mathrm{d}^3 u}{\mathrm{d}y^3} - \alpha^2 \frac{\mathrm{d}u}{\mathrm{d}y} = 0. \tag{19}$$

The boundary conditions (10) and (11) become

$$y=0: \quad \frac{\mathrm{d}u}{\mathrm{d}y}=0, \quad \frac{\mathrm{d}\theta}{\mathrm{d}y}=0, \tag{20}$$

$$y=1: \quad u=0, \quad \theta=0. \tag{21}$$

Using the hydrodynamic conditions (20) and (21), the resolution of Eq. (19) yields the velocity distribution expressed as

$$u=\frac{\alpha[\cosh\alpha-\cosh(\alpha y)]}{\alpha\cosh\alpha-\sinh\alpha}. \tag{22}$$

It is clear that the bulk mean velocity u'_{m} defined as $u'_{\mathrm{m}}=(1/[\varrho(h\times 1)])\int_0^h \varrho u'\,\mathrm{d}y'$ is calculated in dimensionless terms by

$$u_{\mathrm{m}}=\int_0^1 u\,\mathrm{d}y, \tag{23}$$

which equals to unity, using Eq. (22).

Taking into account Eqs. (22) and (23) and making use of boundary conditions for θ, Eq. (17) can be integrated to give the following fully developed temperature profile:

$$\theta=\frac{1}{\alpha(\alpha\cosh\alpha-\sinh\alpha)} \times\left[\frac{\alpha^2}{2}(y^2-1)\cosh\alpha-\cosh(\alpha y)+\cosh\alpha\right]. \tag{24}$$

The average wall friction $\overline{fRe}$ may be considered on the channel centerline at $(y=0)$ such that

$$\overline{fRe}=fRe(y=0)=2[fRe(y=-1)+fRe(y=+1)], \tag{25}$$

where

$$fRe(y=\mp 1)=\frac{\tau_{\mathrm{w}}}{\frac{1}{2}\varrho\overline{u}^2}\frac{\overline{u}h}{\nu}=\pm 2\frac{\mathrm{d}u}{\mathrm{d}y}\bigg|_{y=\mp 1}, \tag{26}$$

where the plus and minus signs correspond to the lower $(y=-1)$ and the upper $(y=+1)$ walls, respectively. Hence, from Eq. (22), the average wall friction can be deduced as

$$\overline{fRe}=\frac{8\alpha^2\sinh\alpha}{\alpha\cosh\alpha-\sinh\alpha}. \tag{27}$$

The substitution of Eq. (22) into Eqs. (15) and (16) then gives directly the pressure variations as follows:

$$-\frac{\partial p}{\partial x}=\frac{\alpha^3\cosh\alpha}{\alpha\cosh\alpha-\sinh\alpha} \tag{28}$$

and

$$\frac{\partial p}{\partial y}=\frac{c}{Da\,Re}\frac{\alpha[\cosh\alpha-\cosh(\alpha y)]}{\alpha\cosh\alpha-\sinh\alpha} \quad (-1\leqslant y\leqslant 1). \tag{29}$$

One can notice immediately that, although both the pressure gradients depend strongly upon anisotropic parameters, it is established that $(\partial p/\partial x\gg\partial p/\partial y)$, since the flow is fully developed along the horizontal axis (x-direction). So, the total pressure loss for the developing flow in the porous duct is

$$\Delta p(x)=\frac{\alpha^3\cosh\alpha}{\alpha\cosh\alpha-\sinh\alpha}x. \tag{30}$$

Moreover, it is seen that, when the porous matrix is isotropic in permeability (i.e., $K^*=1$ $(c=0)$), the pressure gradient in the vertical direction becomes zero and consequently, $\partial p/\partial x=\mathrm{d}p/\mathrm{d}x$, as shown by many authors.

Making use of Eqs. (27) and (30), the criterion of the existence of the fully developed flow follows from the fact that the total pressure drop can be written as

$$\Delta p=\frac{\alpha\coth\alpha}{8}\overline{fRe}\,x. \tag{31}$$

Far from the entrance of the channel, the temperature of the porous medium will be the same as that of the walls (T'_{w}). However, for any finite length and fully developed fields, an invariant local Nusselt number exists (see, for example, [11]). The heat transfer results are given in terms of the Nusselt number for fully developed flow as

$$Nu=4\frac{\left(\partial T'/\partial y'\right)_{y'=h}}{T'_{\mathrm{m}}-T'_{\mathrm{w}}}=\frac{4}{\int_0^1(u/u_{\mathrm{m}})\theta\,\mathrm{d}y} \tag{32}$$

which becomes, using Eqs. (22) and (24), after integration

$$Nu=\frac{48\alpha(\alpha\cosh\alpha-\sinh\alpha)^2}{2\alpha(\alpha^2-9)+15\sinh(2\alpha)+2\alpha(\alpha^2-6)\cosh(2\alpha)}. \tag{33}$$

This result is similar to that found by Nakayama et al. [5] for an isotropic porous situation in which the parameter α is not defined in the same manner.

Two cases of interest will be considered, one with $\alpha\ll 1$ and the other with $\alpha\gg 1$.

Case 1: *The high porosity media*, $\alpha\ll 1(a\ll Da)$. This case corresponds to a weaker anisotropic porous situation for which the resistance resulting from the boundary effects is predominant with respect to that due to the solid matrix, as $Da\to\infty$ when $\alpha\to 0$. This situation approaches to the fluid medium case in which the anisotropic effects of the porous are irrelevant. In this limit, the velocity is given by

$$u=\frac{3}{2}\left(1-\frac{y^2}{2}\right)\left(1-\frac{\alpha^2}{15}\right) \tag{34}$$

and

$$\lim_{\alpha\to 0}u=\frac{3}{2}\left(1-\frac{y^2}{2}\right). \tag{35}$$

From Eq. (27), the average wall friction becomes

$$\overline{fRe} = 24\left(1+\frac{\alpha}{6}\right)\left(1-\frac{\alpha^2}{10}\right). \tag{36}$$

Consequently, as α goes to zero, the limit of the average wall friction is written as

$$\lim_{\alpha\to 0}\overline{fRe} = 24. \tag{37}$$

The pressure gradient and its limit, as α goes to zero, are

$$-\frac{\partial p}{\partial x} = 3\left(1+\frac{\alpha^2}{2}\right)\left(1-\frac{\alpha^2}{10}\right) \tag{38}$$

and

$$\lim_{\alpha\to 0}\left(-\frac{\partial p}{\partial x}\right) = 3. \tag{39}$$

Case 2: *The low porosity media*, $\alpha \gg 1 (Da \ll a)$. This case corresponds to a pure Darcy medium situation in which the anisotropic effects are predominant, as $Da \to 0$ when $\alpha \to \infty$. Then, the velocity distribution is expressed by

$$u = \frac{\alpha}{\alpha - 1}[1 - e^{-\alpha(1-y)}]. \tag{40}$$

The average friction and the pressure gradient are given by

$$\overline{fRe} \approx 8\alpha \tag{41}$$

and

$$-\frac{\partial p}{\partial x} \approx \alpha^2. \tag{42}$$

It is readily found that, as α goes to infinity, the convective heat transfer rate through the channel is calculated by

$$Nu \approx \frac{12e^{2\alpha}}{2+e^{2\alpha}} \tag{43}$$

and

$$\lim_{\alpha\to\infty} Nu = 12. \tag{44}$$

3. Results and discussion

Figs. 2(a) and (b) show, respectively, the horizontal velocity and temperature distributions for only half of the porous duct width when $Da = 4\times10^{-3}$, $\varphi = 0°$ and various values of K^*, using Eq. (22). For each value of K^*, Fig. 2(a) indicates that the velocity at the wall is zero, because according to Brinkman's model, the viscous forces are accounted for and the no-slip condition on the solid wall is satisfied. The velocity increases to a maximum on the channel centerline, the position of which depends upon the value of K^* and drops back to zero at the opposite wall, because of the reason explained earlier. Fig. 2(a) shows that the intensity of the convective flow is promoted with respect to that of an isotropic porous medium corresponding to $(K^* = 1)$, when the permeability ratio K^* is made smaller than one (i.e., $K^* = 10^{-1}$). This is expected, because for a given $Da(< 1)$, i.e., K_1, a value of K^* smaller than unity, when $\varphi = 0°$, corresponds to an increase of the permeability K_2 in the horizontal direction, thus promoting the convective circulation within the channel. Naturally, the reverse trend is achieved when K^* is made large than unity (i.e., $K^* = 10$). Due to the weakness of the strength of the convection motion, the curve is seen to be channeled along the heated horizontal walls, such that thin hydrodynamic boundary layers can be observed in the neighborhood of these walls. The effects of varying K^* on temperature profiles are illustrated in Fig. 2(b). It is

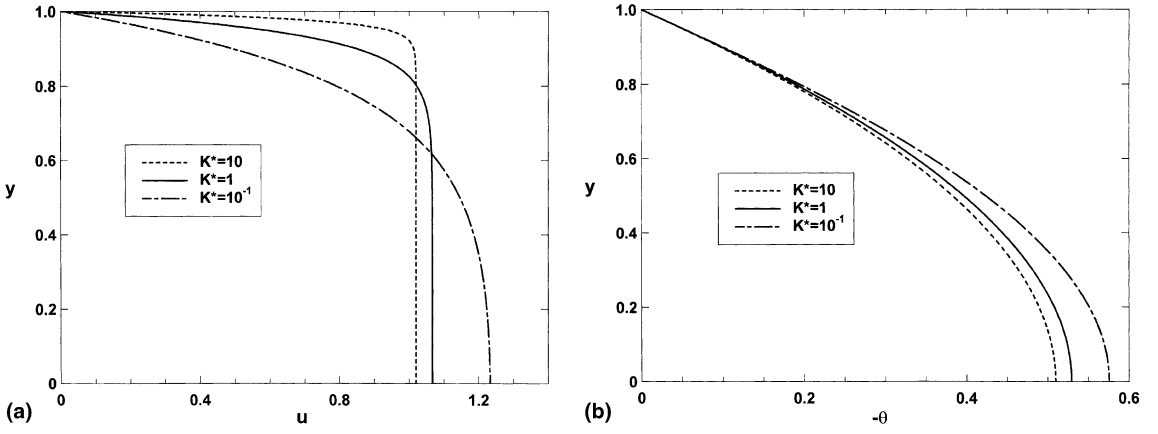

Fig. 2. (a) Effects of the permeability ratio K^* on velocity profile for $Da = 4\times10^{-3}$ and $\varphi = 0°$. (b) Effects of the permeability ratio K^* for on temperature profile for $Da = 4\times10^{-3}$ and $\varphi = 0°$.

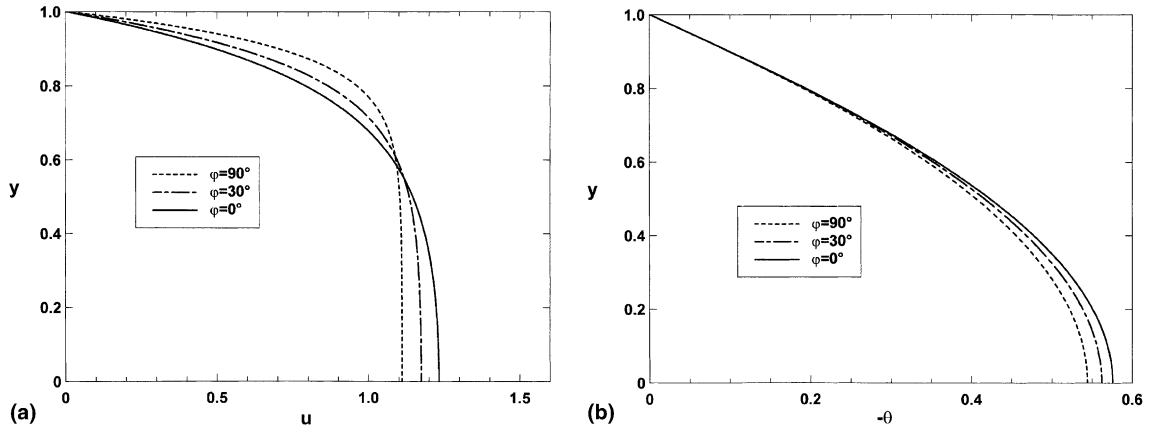

Fig. 3. (a) Effects of the anisotropy angle φ on velocity profile for $Da = 10^{-2}$ and $K^* = 0.25$. (b) Effects of the anisotropy angle φ on temperature profile for $Da = 10^{-2}$ and $K^* = 0.25$.

noticed that the temperature fields have the same behavior described previously for the velocity distribution, revealing that the effect of varying convection in the channel depends strongly on the anisotropic parameters of the porous matrix saturated. As expected, the effect of varying convection causes an increase of the temperature induced within the channel during the heating process, as K^* is made smaller than unity. On the other hand, the convection is favored as the permeability K_2 in the horizontal direction increases when $\varphi = 0°$.

The effects of varying φ, the inclination of the principal axes on the velocity and temperature profiles within the porous duct are presented in Figs. 3(a) and (b), for $Da = 10^{-2}$ and $K^* = 0.25$ (i.e., $K^* < 1$). Because of the forced convection, the entrance velocity imposed forces the circulation of the fully developed flow straight ahead. Accordingly, the velocity and temperature distributions become parabolic and almost uniform, indicating that the saturating convective fluid fills almost the entire section of the channel with a thin boundary layer at each side. Moreover, the results reveal that the convection motion is maximum when $\varphi = 0°$ and minimum when $\varphi = 90°$. For $(K^* > 1)$, the results (not presented here) indicate that the circulation of the convective flow is now maximum when $\varphi = 90°$ and minimum when $\varphi = 0°$. Thus, the convection motion is maximum when the orientation of the principal axis with lower permeability of the anisotropic porous medium is parallel to the gravity. Similar results have been qualitatively reported by Degan and Vasseur [8,12].

In Fig. 4, the average wall friction $\overline{fRe}$ is plotted as a function of Darcy number Da within the porous channel for $\varphi = 45°$ and various values of K^*. Fig. 4 shows that the average wall friction is enhanced when $K^* > 1$ (i.e., $K^* = 5$) and weakened when $K^* < 1$ (i.e., $K^* = 10^{-2}$), in comparison with that of an isotropic porous case for which $(K^* = 1)$. This behavior can be explained by the fact that for a fixed value of Da (i.e., K_1), an increase (decrease) in K^* corresponds to a decrease (increase) of the permeability K_2, i.e., to a weaker (stronger) convective flow, as discussed previously. Darcy's model for the average wall friction predicted by Eq. (41) and plotted in dashed lines in Fig. 4 starts to deviate from Brinkman's model at a Darcy number that decreases as K^* is made weaker. When the Darcy number is made large enough, the results indicate that the curves, for a given value of K^* tend asymptotically toward the pure fluid situation predicted by Eq. (37). The Darcy number required to reach this limit increases as the value of K^* is made higher. For example, this happens at $Da \approx 2 \times 10^{-1}$ when $K^* = 10^{-2}$, and $Da \approx 2$ when $K^* = 5$.

The gradient of the pressure parameter, $(-\partial p/\partial x)$, is plotted in Fig. 5 as a function of Da for $K^* = 2 \times 10^{-1}$ and for various values of φ. It is observed clearly that, when Da is small enough, $(-\partial p/\partial x)$ tends asymptotically toward a value that depends on K^* and φ. The limit

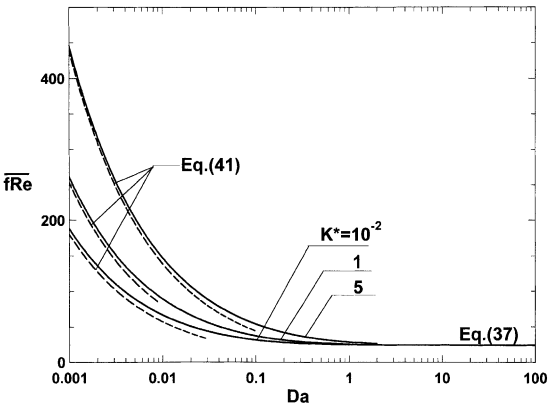

Fig. 4. Effect of the Darcy number Da on the average friction wall for $\varphi = 45°$ and various values of K^*.

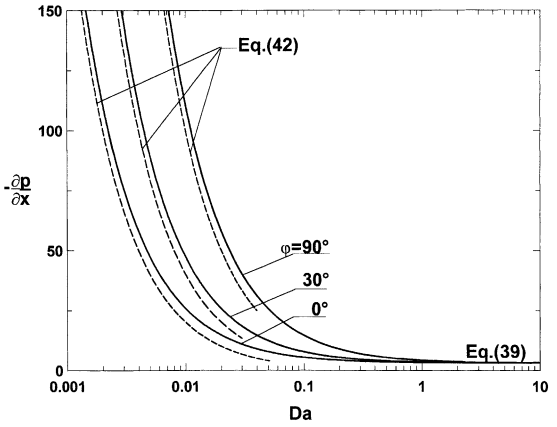

Fig. 5. Effect of the Darcy number Da on the pressure gradient for $K^* = 2 \times 10^{-1}$ and various values of φ.

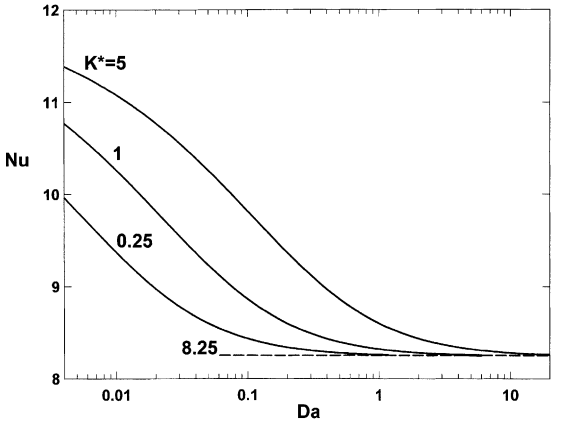

Fig. 6. Effect of the Darcy number Da on the Nusselt number for $\varphi = 0°$ and various values of K^*.

$(Da \to 0)$ corresponds to a pure Darcy medium for which the pressure variation modeled by Eq. (42) is presented as asymptotic curves (dashed lines) for Brinkman's model (solid curves) in Fig. 5. In this limiting case, the effects of varying anisotropic parameters of the porous matrix are observed significant, since $(-\partial p/\partial x)$ decreases as φ is made larger. As expected from Eq. (38), when the permeability of the porous medium Da (i.e., K_1) is increased, the boundary frictional resistance becomes gradually more important and adds to the bulk frictional drag induced by the solid matrix to slow the convection motion. As a result, the effects of varying the anisotropy of the porous medium become less and less important and the present solution approaches that for a pure viscous fluid, Eq. (39). This situation is reached at a Darcy number that decreases as the value of φ is made higher. For example, when $\varphi = 0°$, $Da \simeq 0.3$, and when $\varphi = 90°$, $Da \simeq 2$.

In Fig. 6 the Nusselt number Nu, given by Eq. (33) is plotted as a function of Da for $\varphi = 0°$ and various values of K^*. From Fig. 5, it is clear that, when Da is small enough, the convective heat transfer increases as K^* is made larger. Accordingly, when $K^* = 1$, the result is in agreement with that obtained by Nakayama et al. [5] for the isotropic porous situation. For the pure Darcy medium $(Da \to 0)$, Nu tends asymptotically toward a constant value (not represented here) that does not depend on K^* and φ. As expected from Eq. (43) predicting the heat transfer rate for this limiting case, it is observed that $Nu \to 12$, since $\alpha \to \infty$ (when $Da \to 0$). As Da increases, the effect of anisotropy of the porous matrix becomes less and less important, and the heat transfer within the channel drops progressively toward a constant value. When Da is high enough, i.e., when the resistance resulting from the boundary effects is predominant with respect to that due to the solid matrix, the present solution approaches that for a pure viscous fluid $(Nu \approx 8.25)$ and this, independently of the anisotropy of the porous medium. This situation is reached at a Darcy number that increases as K^* is made larger. For example, for $K^* = 0.25$, $Da \simeq 1.25$ and for $K^* = 5$, $Da \simeq 11$.

Fig. 7 shows the effects of varying the anisotropy orientation φ and Darcy number Da on the Nusselt number for $K^* = 0.25$ and $K^* = 5$. The results indicate that Nu depends strongly on the anisotropy orientation φ of the porous medium. For $K^* = 0.25$, the convective heat transfer is seen to be maximum at 90°, i.e., when the permeability in the vertical direction is maximum, but is minimum at $\varphi = 0°$ and 180°, i.e., when the permeability in the vertical direction is minimum. The inverse is true for $K^* = 5$, for which the heat transfer is now minimum at 90° and maximum at $\varphi = 0°$ and 180°. The fact that for $K^* > 1$ $(K^* < 1)$, Nu is minimum (maximum) at $\varphi = 90°$ and maximum (minimum) at $\varphi = 0°$ and 180°

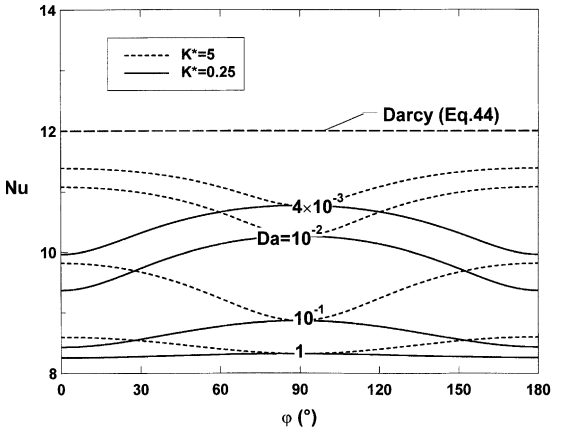

Fig. 7. Effect of the anisotropic angle φ and the Darcy number on the Nusselt number for $K^* = 0.25$ and $K^* = 5$.

can be easily deduced from the first and second derivatives of Nu with respect to φ (Eq. (33)). Thus, it follows from these results that a maximum (minimum) convective heat transfer is reached when the orientation of the principal axis with higher permeability of the anisotropic porous channel is parallel (perpendicular) to the gravity. A similar result has been found while studying convective heat transfer in a vertical anisotropic porous cavity heated from the side isothermally or by a constant heat flux [12–14] . As expected, when Da is small enough, the Darcy's law is represented by a dashed line on the graph. In this limit, the heat transfer is constant ($Nu \approx 12$) and independent of φ. Upon increasing Da, it is seen that, for the reason explained earlier, the heat transfer drops progressively and becomes less and less affected by φ. For example, the case with $Da = 1$ corresponds to a pure fluid situation for which $Nu \approx 8.25$.

4. Conclusion

The purpose in this work was to study the influence of hydrodynamic anisotropy on laminar and fully developing forced convective flow in a parallel-plate horizontal porous channel with heat boundary condition. The porous medium is assumed anisotropic in permeability with its principal axes inclined with respect to the gravity force. The generalized Brinkman-extended Darcy model, which allows the no-slip boundary condition, to be satisfied, is used in the formulation of the problem. Detailed results for the flow fields, temperature distribution and heat transfer rate have been presented in closed form. From this study, the main results are:

1. Both the permeability ratio K^* and the inclination angle φ of the principal axes have a strong influence on the forced thermal convection within the anisotropic porous channel.
2. For the low porosity media ($Da \to 0$), the flow field resembles to that given by a pure Darcy analysis for which the anisotropic effects are predominant. In the limit for high porosity media ($Da \to \infty$), the viscous effects are important and the results become less and less affected by anisotropic parameters.
3. The heat transfer rate within the porous channel is increased as K^* is made larger when $\varphi = 0°$ (i.e., when the permeability in the vertical direction is greater than that in the horizontal direction).
4. A maximum (minimum) heat transfer rate through the porous channel is obtained when the porous matrix is oriented in such a way that the principal axis with higher permeability is parallel (perpendicular) to the gravity.

References

[1] J.C.Y. Koh, R. Colony, Analysis of cooling effectiveness of porous material in a coolant passage, J. Heat Transfer 96 (1974) 324–330.
[2] K.Y. Wang, C.L. Tien, Thermal insulation in flow systems: combined radiation and convection through a porous segment, J. Heat Transfer 106 (1984) 453–459.
[3] J.C.Y. Koh, R.L. Stevens, Enhancement of cooling effectiveness by porous materials in coolant passages, J. Heat Transfer 97 (1975) 309–311.
[4] M. Kaviany, Laminar flow through a porous channel bounded by isothermal parallel plates, Int. J. Heat Mass Transfer 28 (1985) 851–858.
[5] A. Nakayama, H. Koyama, F. Kuwahara, An analysis on forced convection in a channel filled with a Brinkman–Darcy porous medium: exact and approximate solutions, Wärme-und-Stoffübertragung 23 (1988) 291–295.
[6] M. Haajizadeh, C.L. Tien, Combined natural and forced convection in a horizontal porous channel, Int. J. Heat Mass Transfer 27 (1984) 799–813.
[7] T. Nilsen, L. Storesletten, An analytical study on natural convection in isotropic and anisotropic porous channels, J. Heat Transfer 112 (1990) 396–401.
[8] G. Degan, P. Vasseur, Aiding mixed convection through a vertical anisotropic porous channel with oblique principal axes, Int. J. Eng. Sci. 40 (2) (2001) 193–209.
[9] J. Bear, Dynamics of Fluids in Porous Media, Dover Publications, New York, 1972.
[10] G. Degan, P. Vasseur, Boundary-layer regime in a vertical porous layer with anisotropic permeability and boundary effects, Int. J. Heat Fluid Flow 18 (1997) 334–343.
[11] W.M. Kays, M.E. Crawford, Convective Heat and Mass Transfer, McGraw-Hill, New York, 1973.
[12] G. Degan, P. Vasseur, Natural convection in a vertical porous slot filled with an anisotropic medium with oblique principal axes, Numer. Heat Transfer A 30 (1996) 397–412.
[13] G. Degan, P. Vasseur, E. Bilgen, Convective heat transfer in a vertical anisotropic porous layer, Int. J. Heat Mass Transfer 38 (1995) 1975–1987.
[14] X. Zhang, Convective heat transfer in a vertical porous layer with anisotropic permeability, in: Proceedings of the 14th Canadian Congress on Applied Mechanics, vol. 2, 1993, pp. 579–580.